JOURNAL OF MATERIALS SCIENCE 23 (1988) 1851–1860

Temperature dependence of lifetime statistics for single Kevlar 49 filaments in creep–rupture

H. F. WU*, S. L. PHOENIX, P. SCHWARTZ‡
Sibley School of Mechanical and Aerospace Engineering and ‡Department of Textiles and Apparel, Cornell University, Ithaca, New York 14853, USA

Experimental data are presented for the strength and lifetime under constant stress of single Kevlar 49 aramid filaments at two elevated temperatures, 80 and 130° C. As seen in previously published work performed at room temperature (21° C), the strength data could be fitted to a two-parameter Weibull distribution; increasing the temperature caused a decrease in the Weibull scale parameter while the shape parameter remained relatively constant, indicating a decrease in the mean strength but no change in strength variability. Lifetime experiments at both 80 and 130° C were performed at different filament stress levels, ranging from 55 to 92.5% of the Weibull scale parameter for short-term strength at that temperature. These data were fitted to a two-parameter Weibull distribution with large variability (scale parameter values $\leqslant 1$), and evaluated using an exponential kinetic breakdown model in the spirit of Eyring and Zhurkov. Using this model, activation energies in the neighbourhood of 80 kcal mol^{-1} (3.35×10^5 J mol^{-1}) were obtained, suggesting that scission of the C–N bond plays the dominant role in fibre failure at longer times under constant stress.

1. Introduction

One of the major concerns in many of the applications for composite materials is the service lifetime under sustained loads that are significant fractions of the ultimate tensile strength of the material. Experiments carried out on Kevlar† 49–epoxy strands and pressure vessels, such as those at Lawrence Livermore National Laboratory discussed by Phoenix and Wu [1] and Gerstle and Kunz [2], have been both costly and inconclusive, partially as a result of unanticipated problems with UV light degradation and earthquakes. Phoenix and Wu [1], interpreting these data, have shown that both strand tensile strength and lifetime behave in ways not predicted using the simple Rule of Mixtures. Gerstle and Kunz [2] noted that a significant amount of the variability in the lifetime of pressure vessels could be attributed to variation in filament diameters among the spools of yarn used to wind the pressure vessels. It is clear from these results that both spool-to-spool variability and the matrix play important roles, but the roles cannot be determined precisely without first having lifetime data on the individual Kevlar 49 filaments.

Motivated by these findings, Wagner *et al.* [3] studied the statistical variability in the strength and diameter of single Kevlar 49 filaments at room temperature (21° C). The filaments were sampled from two spools supplied by E. I. du Pont de Nemours & Co., Wilmington, Delaware, USA, and taken from the same production lot (No. 74048); the spools hereafter are labelled A and B and are used in the present study. Using the coefficient of variation (c.v. = (standard deviation/mean) × 100%) as a measure, filaments from Spool A were found to have typical variability (10% c.v.) in linear density (mass per unit length), whereas those from Spool B had unusually high variability (25% c.v.). As expected, filaments from Spool B also had much higher variability in failure *load*, but the variability in failure *stress* was virtually identical for the two spools. Studying the lifetime in creep–rupture of these filaments, Wagner *et al.* [4] found that the median lifetime of filaments drawn from Spool B was an order of magnitude larger than that of the filaments drawn from Spool A, when subjected to identical stress levels. However, when the stresses were mormalized by the failure stress of that particular spool, the difference in lifetimes between the spools virtually disappeared. Also the lifetime data for both spools generally fit a two-parameter Weibull distribution, at each stress level, with shape parameter near 0.2. The dependence of lifetime on stress level was studied in the power-law format, and there appeared to be several operating exponents, each corresponding to different time domains, which seemed to agree with those obtained earlier for strands and pressure vessels [1]. These data will be recounted later in the discussion. (This paper [4] also contains, in the Introduction, a discussion of previous theoretical and experimental work in this area.)

Accelerated testing methodologies for composites potentially offer great rewards, and several [5–9] have been proposed to generally forecast long-term mechanical properties. Most of these have relied on time–temperature superposition principles with suitable

* *Present address*: ALCOA Technical Center, Alcoa Center, Pennsylvania 15069, USA.
† Kevlar and Kevlar 49 are registered trademarks of E. I. du Pont de Nemours & Co., Inc.

0022–2461/88 $03.00 + .12

modifications for factors such as moisture. Brinson *et al.* [6] have developed an experimental method that they claim will predict the long-term properties from a short-term (15 min) test, and have used time–temperature superposition to try to predict the lifetime of organic fibre composites [7]. Springer [9] developed a model for predicting the mechanical properties of composites at elevated temperatures that can be used to calculate changes in the tensile, compressive, and shear strengths and moduli as functions of exposure time. These models are primarily deterministic and have not been extensively proven in the setting of long-term lifetime.

In the past, few experimental studies have been performed that contain a full statistical treatment of the creep–rupture of both a fibre and a composite made from this fibre. At the same time, predictive reliability models are being developed that rely on these data, and thus experimental results are much in need. This paper presents just such results for single Kevlar 49 filaments.

In experiments closely related to those considered here, Chiao and co-workers [10, 11] performed a study of the creep–rupture lifetime of epoxy-impregnated Kevlar 49 strands at temperatures between 100 and 120° C, and stress levels between 67 and 80% of short-term strength. A modified Arrhenius model attributed to Zhurkov and further modified to include Weibull statistics was used to fit the data. They determined a stress-free activation energy of 36.6 kcal mol^{-1} (1.52×10^5 J mol^{-1}) and a time constant of 2.84×10^{-7} sec. With moderate success, the model was used to predict the lifetime of strands at 25° C for which results were previously available. Using the same equipment, Penn [12] and Penn and Sherry [13] further considered the creep–rupture lifetime of strands at 56% of short-term strength. They concluded that modifications to the previous models were needed.

In other experiments, Gerstle and Kunz [2] found that the failure time of pressure vessels as a function of the applied pressure followed a power-law relationship, and stressed the need for careful control of pressure (or stress) level both in composite vessel design as well as for creep–rupture experiments. Cook *et al.* [14] studied creep in aramid yarns with special emphasis on wet (immersed) and hot (65° C) conditions. They reported decreases in reaction rates with increasing stress, but increases with the presence of water, a fact that they attribute to effects on secondary bonding that do not have a "great bearing on stress–rupture behaviour". Lafitte and Bunsell [15] subjected single Kevlar 29 fibres to a variety of tensile cyclic and static loading conditions, attributing failure at shorter lifetimes to fatigue and failure at longer lifetimes to creep. They reported no differences in fracture morphology among samples failed by simple tension, fatigue, or creep; all samples showed the complex splitting characteristic of aramid fibres.

With respect to molecular kinetics and mechanisms of failure, two competing models, chain slippage and chain scission, have been proposed at various times. Coleman and co-workers [16–18] developed a slippage model and used it to explain creep–rupture in nylon fibres. Wilfong and Zimmerman [19] proposed this model for creep–rupture in Kevlar fibres. The underlying theory for these models was built upon the rate-process formulations given by Eyring [20] and Tobolsky and Eyring [21].

Scission models seem to stem from the work of Tobolsky and Eyring [21] and, later, Coleman [22]. Similar kinetic models were later proposed by Zhurkov [23] and Zhurkov and Korsukov [24], and also extended to include local stress effects in the polymer network [25, 26]. Henderson *et al.* [27] have pointed out that it is difficult to distinguish between the parametric forms of the chain-slippage and chain-scission models, especially as regards lifetime data.

Christensen and co-workers [28–31], following the spirit of classical fracture mechanics, have proposed a viscoelastic kinetic formulation of the classical crack stability problem in fracture mechanics, and have applied it to the creep–rupture lifetime of polymers, including Kevlar 49–epoxy composites [29, 31].

In the present work we report the results of strength and creep–rupture experiments performed at elevated temperatures (80 and 130° C) on single Kevlar 49 filaments. These data complement and extend the earlier work of Wagner and co-workers [3, 4] and hold out the promise both of developing accelerated testing routines and of providing data for their evaluation and refinement.

2. Theoretical framework

For the experiments discussed later, we consider a theoretical framework largely initiated by Coleman [16–18, 22], and further developed by Phoenix and co-workers [4, 32–35]. We consider only a few selected results, referring the reader to the above works for details. We consider two formats, namely the exponential breakdown rule and the power-law breakdown rule as originally named by Coleman.

2.1. Creep–rupture lifetime

Considering first the creep–rupture lifetime of single filaments under constant stress L, the distribution function for lifetime is of the Weibull form

$$F(t) = 1 - \exp\{-[\kappa(L)t]^s\} \qquad t \geqslant 0 \qquad (1)$$

where s is the Weibull shape parameter for lifetime and $\kappa(L)$ is the breakdown rule. In the case of the exponential breakdown rule, $\kappa(L)$ is given by

$$\kappa(L) = \alpha \exp(\beta L) \qquad (2)$$

where α and β are positive constants. Connecting these constants to molecular events, a convenient interpretation is that

$$\kappa(L) = \tau_0^{-1} \exp[-(U_0 - \gamma L)/kT] \qquad (3)$$

where U_0 is the stress-free activation energy associated with the underlying molecular failure events, γ is the activation volume (which may include stress concentration effects), k is Boltzmann's constant, T is the absolute temperature and τ_0 in the simplest interpretation is a bond vibration period. Thus the constants in Equation 1 become $\alpha = \tau_0^{-1} \exp(-U_0/kT)$ and $\beta = \gamma/kT$. Using this law, the lifetime distribution

function may be written in the conventional Weibull form

$$F(t) = 1 - \exp[-(t/r)^s] \qquad t \geqslant 0 \qquad (4)$$

where the Weibull scale parameter r is given by

$$r = \tau_0 \exp[(U_0 - \gamma L)/kT] \qquad (5)$$

This result is of the same form as that attributed to Zhurkov [23, 24]. Note that strength plotted against lifetime in semi-log coordinates (L against log r) is linear, with slope and intercept determined by α and β. Thus, varying the temperature T allows for the determination of the quantities U_0, γ and τ_0 in a fairly straightforward manner.

In the format of the power-law breakdown rule, we have

$$\kappa(L) = \mu L^{\varrho} \qquad (6)$$

where μ and ϱ are positive constants. Thus

$$r = \mu^{-1} L^{-\varrho} \qquad (7)$$

This rule is considered in more detail in Wagner *et al.* [4] and Phoenix and co-workers [32–34]. There, it is argued that

$$\varrho = \tilde{U}_0/(kT)$$

and

$$\mu = \tau_0^{-1} \tilde{\sigma}_0^{-\tilde{U}_0/kT}$$

based on molecular considerations, where $\tilde{U}_0$ is related to the stress-free activation energy and $\tilde{\sigma}_0$ is related to the theoretical bond strength. Note that strength against lifetime on log–log coordinates (log L against log r) plots as a straight line with a negative slope $1/\varrho$. Thus varying the temperature T allows for the determination of $\tilde{U}_0$, $\tilde{\sigma}_0$ and τ_0 in a fairly straightforward manner.

2.2. Short-term strength†

Turning to short-term strength under the power-law format, the resulting distribution function for filament strength is given by the Weibull distribution

$$F^*(x) = 1 - \exp[-(x/a)^b] \qquad x \geqslant 0 \qquad (8)$$

where the positive constants a and b are the Weibull scale and shape parameters, respectively. These parameters are in turn given by $b = s(\varrho + 1)$ and $a = [R(\varrho + 1)/\mu]^{1/(\varrho+1)}$ where R is the loading rate [4]. Thus, according to the model, the Weibull parameters for strength and lifetime are connected. For example, suppose the Weibull scale parameter for strength a is known at stress rate R and we want to forecast the Weibull scale parameter for lifetime r at the stress level $L = a$. This is determined [4] to be $r = a/[R(\varrho + 1)]$, which is the time required in the tension test to reach the stress a divided by $(\varrho + 1)$. Using this idea, results from tension tests can be converted to lifetime results for comparison, as is done later.

Under the exponential breakdown rule, one does not obtain a Weibull distribution function for strength as was first pointed out by Coleman [22]. (See Phoenix [35] for a summary.) Instead the resulting distribution function is approximately (for $\exp(\beta x) \gg 1$) the double exponential distribution function

$$F^*(x) \cong 1 - \exp\{-[\alpha(\beta R)^{-1} \exp(\beta x)]^s\} \qquad x \geqslant 0 \qquad (9)$$

Since this form is inconvenient for our purposes, we do not use it as the primary tool in our later analysis of the filament strength data. Fortunately the two distributions of Equations 8 and 9 give similar graphical plots and predictions for suitably chosen values of the various parameters. Also, the prediction of lifetimes from strength results may be accomplished in this setting also. For example, if the median strength L' at a given loading rate is known the median lifetime t' at a stress level equal to L' is simply the median time to failure in the tension test divided by $\beta L'$.

More generally, Phoenix [35] has compared the two formats for representing results when $\varrho \gg 10$, and for a limited load range about some level L_m the two formats give similar numerical predictions and plots with the connection

$$\varrho \cong \beta L_m$$

and

$$\mu \cong \alpha \exp(\varrho) L_m^{-\varrho}$$

Indistinguishability is often found to be the case in lifetime experiments in materials when one is trying to choose between the two formats solely on the basis of experimental data. In the present setting, wide variations in load level and temperature reveal basic differences in the two models, as we note later.

3. Experimental procedures

As mentioned previously, the two spools of Kevlar 49 yarn, identified earlier as Spools A and B, were also used in the present study to obtain specimens for testing. The use of the same material throughout gives added validity to the inferences drawn from the experimental results. Also, because filament tabbing procedures were identical for both strength and creep–rupture experiments, all specimens (~ 1500 from each spool) were prepared in advance and selected at random for both the strength and creep–rupture experiments, providing added insurance against biased results from sample preparation variabilities, or variabilities existing along the length of a yarn (which are observed).

The tabbing procedures generally followed those outlined previously [4] with filaments mounted on light cardboard tabs using an epoxy cement. Prior to testing, the central portion of the tab was cut away, leaving a filament of gauge length 50 mm to be tested.

Because the testing was to be carried out at elevated temperatures, and, for creep–rupture, over a long time period, care was taken in the selection of an adhesive system. Preliminary tests of various epoxies indicated that outgassing during high-temperature curing could cause a strength reduction in the fibres,

† Throughout the remaining discussion, the terms "strength" and "failure stress" will be used interchangeably.

and lead to erroneous results. Another result of these preliminary tests was that some of the bonding systems, while not affecting the filament *strength* (Weibull scale parameter), did substantially affect the strength *variability* (as evidenced by changes in the Weibull shape parameter), and these systems too were rejected for use. We finally selected Omegabond® 101 (Omega Engineering, Inc., Stamford, Connecticut, USA) for use in mounting the fibres; this epoxy system is rated for continuous use to 135° C, and is fully cured after 24 h at room temperature. This system, we feel, was very acceptable as few specimens failed at the tabs during testing.

Single filaments approximately 120 mm in length were selected at random from the yarn. Approximately 50 mm from each filament was used to measure the cross-sectional area using the vibroscope method (ASTM D1577-79), and the remainder was mounted on the cardboard tab. It has been shown [3] that it is important to measure the area of each filament and to use that area when calculating failure stress; using one average value for all specimens may provide misleading results.

3.1. Short-term strength

To determine the distribution for short-term strength, samples were tested in tension using an Instron model TM (constant rate of extension) machine fitted with an environmental chamber; sample sizes of fifty were used in all cases. The samples were tested at a strain rate of 0.1 min^{-1}, and gauge lengths of 50 mm were used. (Typically, we found a strain to failure of approximately 0.023 resulting in a total testing time of 14 sec.) For completeness, tests were performed at four different temperatures: 21, 80, 130 and 180° C. In addition, at 21° C we also performed tension tests at strain rates of 0.004, 0.02, 0.04, 0.1 and 0.4 min^{-1} on a different set of filaments drawn from both spools in an attempt to look at the behaviour of filaments at very short failure times.

3.2. Creep–rupture lifetime

A specially built creep–rupture frame [4] was used for the tests. This frame had microprocessor timing, and was capable of monitoring 48 simultaneous creep–rupture experiments, although due to occasional breakage during mounting or switch malfunction some runs contained fewer than 48 samples. The frame was placed in a large forced-air oven, and special precautions were taken to suppress vibrations and shield the specimens from air currents. Filament loading was done using dead weights.

In the determination of the applied load for each different test temperature, the values for strength determined at that particular temperature were used. For tests conducted at 80° C, stress ratios of 60, 65, 70, 80, 85, 90 and 92.5% of the Weibull scale parameter for short-term strength were selected; at 130° C, stress ratios of 55, 60, 70, 75, 80, 85, 90 and 92.5% were used. As the cross-sectional area of each filament had been determined earlier, the loading weight suspended from a given filament was individually tailored so that each filament saw the same stress as all others at that ratio; in other words, larger-diameter filaments were loaded with a larger weight than smaller-diameter filaments at a given stress ratio.

TABLE I Statistics for linear density, failure load and failure stress of filaments at various temperatures

Spool	Temperature (° C)	Linear density* ($mg\,m^{-1}$); (% c.v.)	Failure load (N); (% c.v.)	Failure stress (MPa); (% c.v.)
A	21	0.1649	0.386	3376
		(8.63)	(13.99)	(11.62)
	80	0.1651	0.361	3144
		(7.72)	(14.94)	(11.94)
	130	0.1660	0.331	2876
		(8.69)	(13.63)	(11.43)
	180	0.1622	0.310	2750
		(9.67)	(14.44)	(10.61)
B	21	0.1750	0.417	3428
		(24.33)	(27.22)	(11.17)
	80	0.1763	0.396	3231
		(28.75)	(32.31)	(11.02)
	130	0.1685	0.338	2895
		(25.31)	(26.86)	(11.59)
	180	0.1848	0.337	2623
		(31.54)	(33.95)	(10.93)

*Measured at 21° C, 65% relative humidity.

The creep–rupture experiments were run typically for 168 h, at which time the tests were censored (Type I censoring), if indeed survivors remained. During the test the oven windows were covered as an added precaution against possible effects of UV radiation from the overhead lights. As an additional precaution to remove testing bias, each testing run was constructed using filaments from both spools.

4. Results and discussion

4.1. Short-term strength

In Table I are presented the means and coefficients of variation of linear density ($mg\,m^{-1}$), failure load (N) and failure stress (MPa) results for each spool at each temperature (note that the values for linear density were obtained at room temperature); the Weibull shape and scale parameters for strength, determined using the method of maximum likelihood estimation (MLE), are presented in Table II. Figs 1 and 2 are Weibull probability plots of the data at 80 and 130° C, respectively, with the results from both spools at each temperature being given on the same plot. The lines fitted through the data for each spool are determined from the MLE of the shape and scale parameters,

TABLE II MLE of the Weibull shape ($\hat{b}$) and scale ($\hat{a}$) parameters for filament strength at various temperatures

Spool	Temperature (° C)	$\hat{b}$	$\hat{a}$ (MPa)
A	21	10.2	3538
	80	10.1	3304
	130	10.5	3019
	180	10.7	2879
B	21	10.4	3594
	80	10.2	3385
	130	10.1	3041
	180	10.2	2751

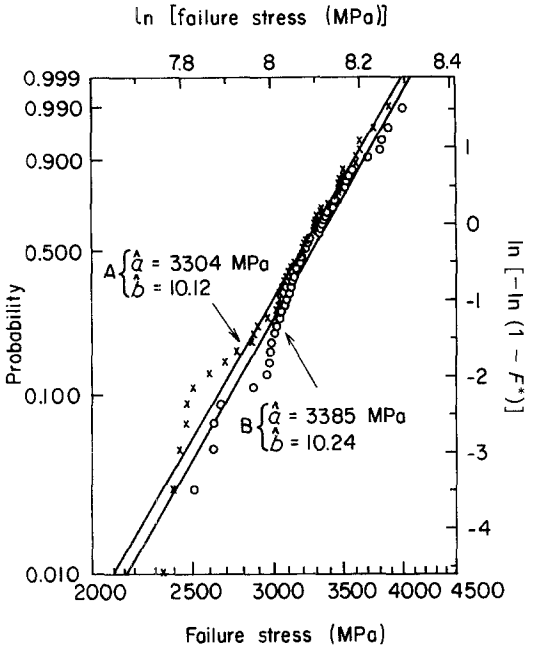

Figure 1 Weibull probability plots for filament failure stress for (x) Spool A and (o) Spool B at 80° C and strain rate 0.1 min^{-1}.

indicated by the circumflex (^) over the letter. First turning to the figures, we see that the data are generally well fitted by the Weibull distribution, indicating that the Weibull nature of filament strength holds over a range of temperatures. From Table I we see that much of the variability in failure load can be explained by the variability in linear density, as the variability in failure stress is virtually identical for both spools, although filaments drawn from Spool B have a significantly higher variability in linear density overall (for a discussion of the effects of variability on failure stress, see Appendix B in Wagner *et al.* [3]). We also see from this table the importance of using the linear density of each filament to calculate the failure stress, for if we were to simply use an average value, then we

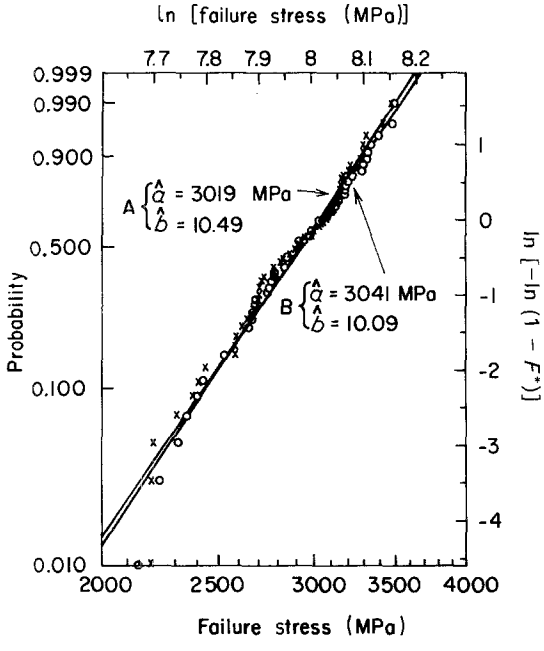

Figure 2 Weibull probability plots for filament failure stress for (x) Spool A and (o) Spool B at 130° C and strain rate 0.1 min^{-1}.

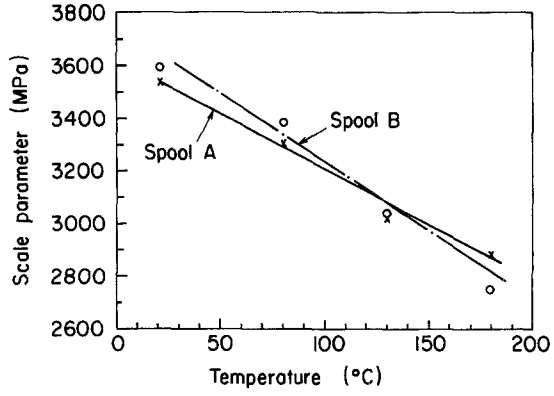

Figure 3 Correlation between filament failure stress and temperature for (x) Spool A and (o) Spool B.

would conclude that the variability in stress was different for the two spools, as we would, in effect, be comparing failure load instead of stress.

Fig. 3 plots the scale parameters for strength as a function of temperature as obtained from Table II. The observed strength reduction of Kevlar 49 with increasing temperature has been reported previously [19]. Note, however, that the variability remains remarkably constant with temperature as is reflected in the near-constant values of the Weibull shape parameter. Using the method described in Section 2.2, we will later convert these results to lifetime estimates to be compared with the actual lifetime results.

4.2. Creep–rupture lifetime

In Tables III and IV we present the MLE results for lifetimes of filaments drawn from Spools A and B and taken at 80 and 130° C, respectively, with r representing the scale parameter, s the shape parameter and (^) indicating that the values are the maximum likelihood estimates. Typical Weibull plots are given in Figs 4 to 7 for different values of the stress ratio, with the number of filaments N_0 that failed immediately upon application of the load and, when appropriate, the number surviving N_c at the time of censoring. All specimens tested at 130° C failed prior to the predetermined censoring time. For Spool A at 80° C, 2, 38, 56 and 96% of the specimens survived at 80, 70, 65 and 60% stress ratios, respectively; for Spool B, 18 and 43% survived at 70 and 65% stress ratios, respectively. Using the results for short-term strength, we could predict the number of filaments that we would expect to fail upon initial loading for each test. The actual and predicted numbers of "initial failures" were very

TABLE III MLE of the Weibull scale ($\hat{r}$) and shape ($\hat{s}$) parameters for filament lifetimes at 80° C

Stress ratio (%)	Spool A			Spool B		
	$\hat{r}$ (h)	$\hat{s}$	Median (h)	$\hat{r}$ (h)	$\hat{s}$	Median (h)
92.5	–	–	–	0.032	0.39	0.012
90	0.317	0.38	0.043	0.058	0.37	0.050
85	0.594	0.29	0.167	0.129	0.41	0.053
80	2.09	0.29	0.591	0.804	0.39	0.311
70	196	0.38	75.3	64.5	0.29	18.2
65	1077	0.30	314	374	0.29	105

TABLE IV MLE of the Weibull scale ($\hat{r}$) and shape ($\hat{s}$) parameters for filament lifetimes at 130° C

Stress ratio (%)	Spool A			Spool B		
	$\hat{r}$ (h)	$\hat{s}$	Median (h)	$\hat{r}$ (h)	$\hat{s}$	Median (h)
92.5	0.026	0.35	0.009	–	–	–
90	0.046	0.38	0.017	0.025	0.49	0.012
85	0.200	0.41	0.081	0.112	0.46	0.051
80	0.420	0.47	0.193	0.240	0.46	0.109
75	1.19	0.48	0.878	0.501	0.47	0.299
70	5.73	0.50	2.74	2.34	0.51	1.15
60	33.4	0.78	20.9	16.5	0.67	9.56
55	93.2	0.99	64.4	78.3	1.03	54.9

close, and we took this as an indication that our loading scheme was not influencing our results at very short lifetimes.

As was done by Wagner *et al.* [4], we investigated the residual strength of filaments that survived to the censoring time by testing them in tension after censoring the lifetime experiment. These results are presented in Table V. There seems to be generally a 5 to 10% strength reduction in the surviving filaments when compared with the initial mean strength at that temperature. The strength degradation process is extremely complex and difficult to model in general, although Wagner *et al.* [4] have provided an analysis within the power-law framework. Generally we find that the results were not well modelled by this method, probably because of basic differences in scaling between short-term strength and long-term life as discussed later.

The results given in Tables III and IV show significant differences in lifetimes at each stress level between filaments from the two spools. It may be noted that filaments from Spool A consistently have greater lifetimes than filaments from Spool B, for both absolute stress and stress ratios. This would seem

TABLE V Residual strength of filaments surviving 168 h at 80° C

Spool	Stress ratio (%)	Number surviving	Residual strength (%)*
A	70	16	94.31
A	65	23	89.70
A	60†	23	93.02
B	65	19	94.58

*Percentage of initial mean strength at 80° C.
†Only one failure occurred and this was during loading.

to indicate that there may be structural differences between the fibres drawn from the two spools, possibly a skin–core effect which, because of the higher variability in filament size (and hence skin-to-core ratio) in Spool B, manifests itself as differences in lifetime. Variability in lifetimes at 80° C seems not to be affected by differences in stress level, as seen in Fig. 8, which shows the measured Weibull shape parameters. (The variation in the shape parameter is well within the experimental error.) This is not true for the data at 130° C, also shown in Fig. 8, where the variability can be seen to decrease significantly (increasing Weibull shape parameter) with decreasing stress level. That both spools show consistent results at each temperature would seem to rule out filament size variability as the cause of this effect, indicating that it is indeed due to stress level and temperature. We comment further on these results later.

In Fig. 9 we have plotted the stress level against the logarithm of the Weibull scale parameter for lifetimes appropriate to the exponential breakdown rule format as described earlier. Also included are the lifetime results for room temperature as obtained by Wagner *et al.* [4]. (In the latter case, the stress levels for Spool A were adjusted upward by about 7% to compensate for the somewhat lower strength and correspondingly lower lifetimes observed for filaments extracted from

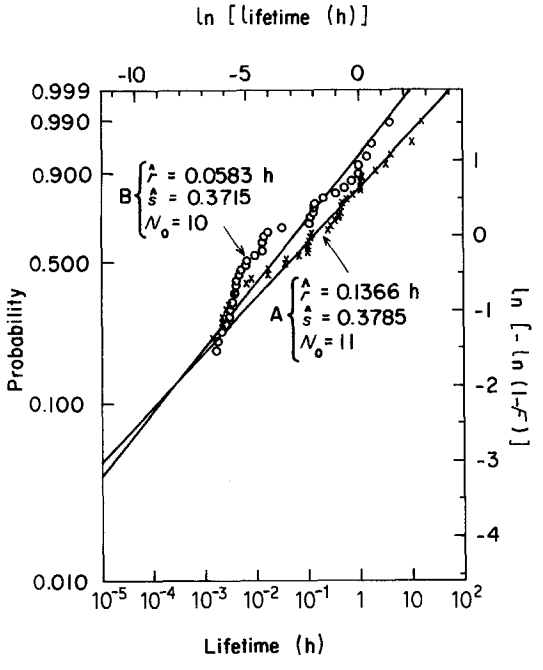

Figure 4 Weibull probability plots for the lifetimes of filaments from (x) Spool A and (○) Spool B at 90% stress ratio and 80° C.

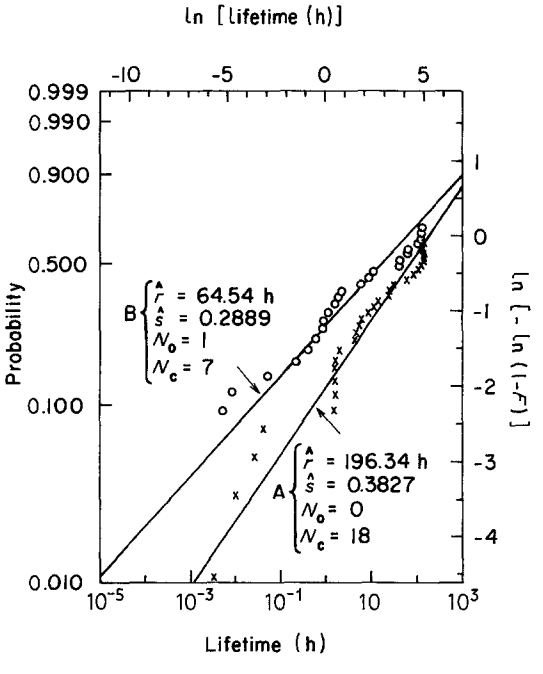

Figure 5 Weibull probability plots for the lifetimes of filaments from (x) Spool A and (○) Spool B at 70% stress ratio and 80° C.

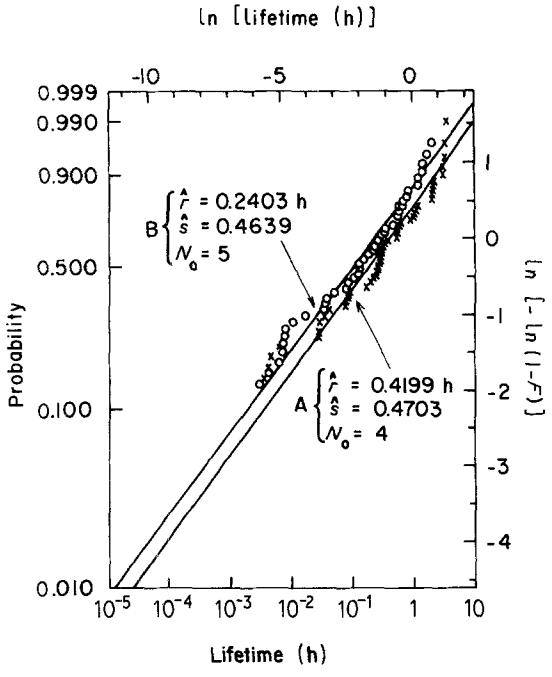

Figure 6 Weibull probability plots for the lifetimes of filaments from (x) Spool A and (○) Spool B at 80% stress ratio and 130° C.

that particular position along the spool. Specimens for the present study were taken from much farther into the spool.) We fitted Equation 5 to the lifetime data using a least-squares algorithm conditioned on all lines projecting to the point of intersection of the lines for the 80 and 130° C data, as shown in Fig. 9. Depending on the pair of lines (temperatures) used to solve for the various quantities, we calculated activation energies U_0 varying from 76.8 to 82.7 kcal mol^{-1} (3.21×10^5 to 3.46×10^5 J mol^{-1}). An acceptable overall fit is obtained by taking $U_0 = 80$ kcal mol^{-1} (3.35×10^5 J mol^{-1}), $\gamma = 0.208$ nm^3 and $\tau_0 = 0.067$ sec. The above activation energy is consistent with that quoted [32] for the C–N bond in Kevlar 49 fibres. The

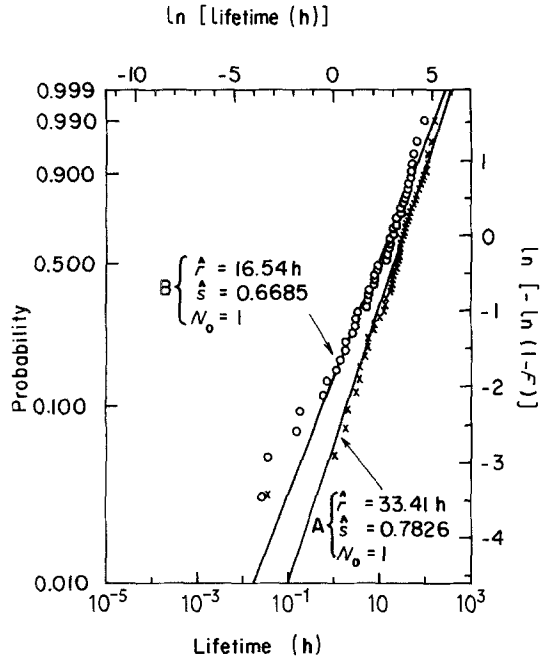

Figure 7 Weibull probability plots for the lifetimes of filaments from (x) Spool A and (○) Spool B at 60% stress ratio and 130° C.

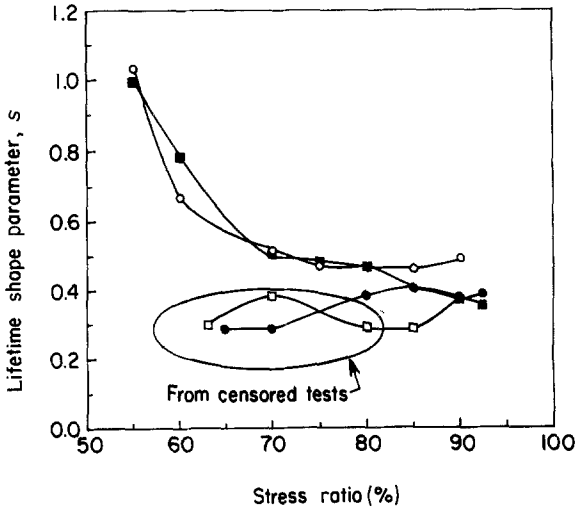

Figure 8 Effect of stress ratio on Weibull shape parameter for lifetimes of filaments: (□) Spool A, 80° C; (●) Spool B, 80° C; (■) Spool A, 130° C; (○) Spool B, 130° C.

activation volume is approximately that of the unit cell in Kevlar 49, though the value does seem to reflect stress concentration effects. However, the value of the time constant τ_0 is not easily explainable as it is ten orders of magnitude larger than the 10^{-12} seconds usually taken as the bond vibration period. Later we comment on possible explanations.

With respect to Fig. 9, it is of interest to note that for Spool A at 80° C and the 60% stress level only one filament of the 24 tested had failed by the censor time of 240 h, and this one failed on loading. Thus we cannot calculate a scale parameter value. However, using the 80° C plot in Fig. 9 we predict a lifetime scale parameter value of about 10 000 h, and using a shape parameter value of 0.35 as suggested by Fig. 8 we predict about six failures by the censor time. Indeed the actual number of failures was only one, suggesting that the actual scale parameter value at this lowest stress level (1980 MPa) lies to the right of the 80° C line in Fig. 9; that is, there is no evidence of a "downturn" in the curve.

The above results are very different from those obtained by Chiao and co-workers [10, 11] for Kevlar 49–epoxy strands. As mentioned earlier, they obtained a much smaller activation energy $U_0 = 36.3$ kcal mol^{-1} (1.52×10^5 J mol^{-1}) and activation volume $\gamma = 0.018$ nm^3 and time constant $\tau_0 = 2.84 \times 10^{-7}$ sec, which though smaller than our value is still far short of the bond vibration period 10^{-12} sec. It should be pointed out that in their experiments both the temperature range (100 to 120° C) and the stress range (67 to 80%) were limited compared with those in our case. While they assumed the matrix to play a minor role in their experiments, it was close to its glass transition temperature and probably prone to creep around fibre breaks, thus introducing time-dependent load-sharing effects. The comparison between their results and ours perhaps underscores the need for basic data on single filaments in order to separate fibre effects from matrix effects.

In Fig. 10 we show the predicted values of the lifetime scale parameter based on the values for the strength scale parameter of Table II. These values

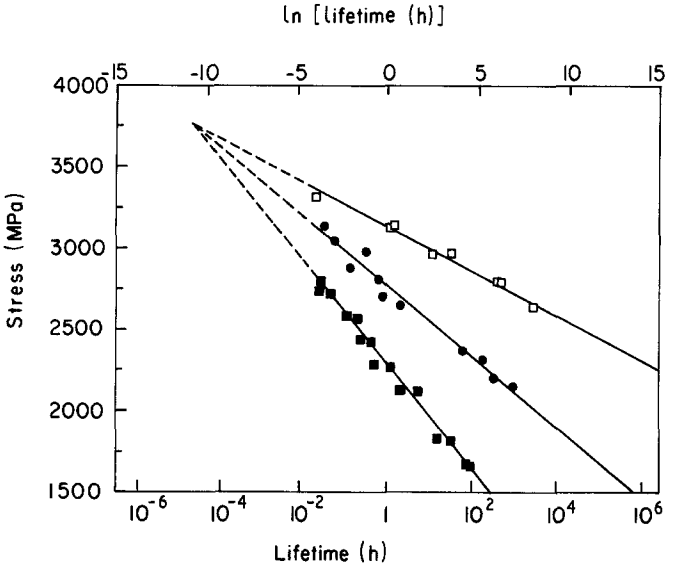

Figure 9 Stress level against ln (lifetime) for filaments from Spools A and B: (□) 21° C (scaled) from [4]; (●) 80° C, (■) 130° C (this work). $U_0 \cong 3.35 \times 10^5\,\mathrm{J\,mol^{-1}}$ (80 kcal mol^{-1}), $\tau_0 = 0.067$ sec, $\gamma = 0.208\,\mathrm{nm^3}$.

were computed using the method outlined in Section 2.2. Clearly the results based on short-term strength do not fit in with those for long-term life on this format, lying far to the left. (There is reasonable agreement if the calculated lifetimes are taken as the time of the tension test, which is about 14 sec, but this time is surely far too long since a very small fraction of this time is spent at a load level producing short-term creep–rupture.) Also in Fig. 10 we have sketched in lines which represent the behaviour we would expect if our creep–rupture equipment had sufficient resolution to conduct experiments at such high stress levels and short times. The line at 21° C is actually based on experimental results from the previously mentioned tension tests at various strain rates ranging from 0.4 to 0.004 min^{-1}. Over this two-decade range we found no measurable drop in strength as indicated by the flatness of the line as drawn. From these results we conclude that the molecular mechanisms for short-term strength are significantly different from those for long-term lifetime, possibly involving a complex interaction of both chain scission and slippage.

Wilfong and Zimmerman [19] used the chain-slippage model of Coleman and co-workers [16–18] to explain creep–rupture in Kevlar. From a linear plot of strength against temperature, they extrapolated to a zero-strength temperature T_0 of 640° C. From the data in Table II and Fig. 3 we obtain approximately 800° C for T_0 by the same method — note that Kevlar 49 decomposes at 482° C, thus the analyses here and in Wilfong and Zimmerman [19] are only valid for determining the relevant energies. (Their results appear to be for yarns, which were almost 20% lower in strength.) Proceeding with their calculation of the energy of activation — which amounts to using Equation 5 with $r = 1$ sec, $\tau_0 = 10^{-12}$ sec and $L = 0$ — we calculate 60 kcal mol^{-1} (2.5×10^5 J mol^{-1}) in our case to compare with 48 kcal mol^{-1} (2.0×10^5 J mol^{-1}). Neither value corresponds to the 80 kcal mol^{-1} value we obtained for the lifetime experiments. These disparities are perhaps not surprising when we recall from Fig. 10 that the strength and lifetime results follow quite different patterns. Apparently, by these methods, short-term strength is not a good predictor of long-term life.

Fig. 11 [36] shows a plot of the Weibull scale parameter values for lifetime using the power-law format. Also included are the predicted lifetime values

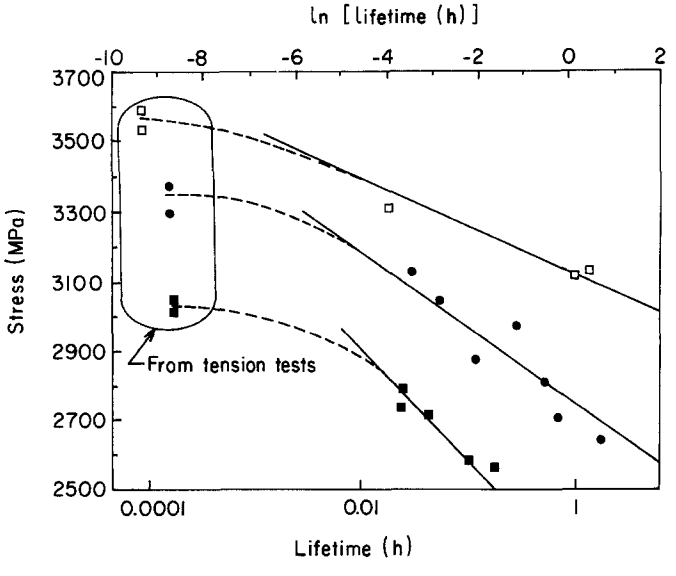

Figure 10 Stress level against ln (lifetime) in the short-time region with tensile test results, scaled and unscaled, included: (□) 21° C (from [4]); (●) 80° C, (■) 130° C (this work).

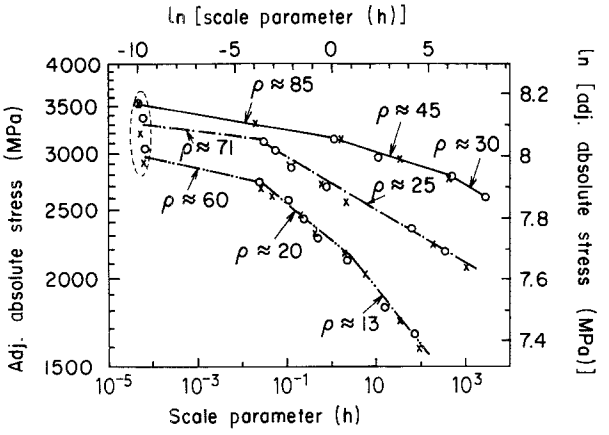

Figure 11 ln (stress level) against ln (lifetime) for filaments from (x) Spool A and (○) Spool B: (——) 21° C (from [4]); (–·–·–·–) 80° C, (–··–) 130° C (this work). Points enclosed by a dashed line are from tension tests.

calculated from the short-term strength results. The power-law exponent ϱ is the inverse of the (negative) slope on this scaling. (To enhance the display of the data all on one graph we rescaled slightly the absolute stress levels for Spool A relative to those for Spool B at all temperatures.) Despite arguments given by Phoenix and co-workers [32–34] supporting its use, it is clear that the power-law format is not particularly successful at resolving the lifetime data for Kevlar 49; that is, ϱ varies with the stress level. A major difficulty may be the wide stress range that is involved as the temperature increases, and this may invalidate the approximations made in the molecular modelling especially at the lowest stress levels. In any event neither the exponential nor the power-law format is able to resolve the results at the highest stress levels. We are working on an extension of the modelling by Phoenix and co-workers [32–34] in the context of the exponential breakdown rule. The tasks are to explain the anomalies in the strength and lifetime data at the highest stress levels and the large time-constant value τ_0 which was experimentally determined. Preliminary indications are that molecular stress redistribution in the model yields complex changes in a key quantity which plays the role of the time constant.

Returning to Fig. 8, we mention that at 80° C an increase in the Weibull shape parameter s with a further decrease in stress level L is possible if longer-term experiments ($\sim 10\,000$ h) are conducted. Two pieces of evidence suggest this possibility. First, we recall that at the 60% stress level a value of $s = 0.35$ leads to *six* predicted failures out of 24, before 240 h, rather than the *one* we observed. To predict a single failure, $s \cong 0.8$ is required. Second, under the power-law breakdown format we earlier had $s = b/(\varrho + 1)$. Taking $b = 10$ (Table II) and ϱ values from Fig. 11, we compute $s = 0.38$ for 80° C at all stress levels tested, whereas for 130° C we have $s = 0.48$ at high stress levels rising to 0.71 at low stress levels. These observations are quite consistent with the results plotted in Fig. 8. Note that downward curvature and a decrease in ϱ must be expected in Fig. 11 at 80° C as the stress is decreased further (which is consistent with a linear plot on Fig. 9). In fact from $\varrho \cong \beta L_m$, ϱ should decrease with L_m and s should increase as $1/L_m$.

In order to learn more about failure modes of the single filaments, the topography of the fracture surface was studied. Previously, Lafitte and Bunsell [15] had reported no difference in fracture morphologies between fibres failed in simple tensile fatigue or in creep, all exhibiting fibrillation. In our tests, filaments that failed in creep after very short time periods (< 3 min) seemed to have failed through transverse crack propagation; over one or two fibre diameters along the fibre, no long-range splitting or fibrillation was observed. Filaments that failed after longer periods (> 100 h) exhibited the splitting and fibrillation characteristic of Kevlar. This splitting does not preclude chain scission as the key initiating mechanism, since splitting may only predominate in the failure surface after crack instability has been reached.

Finally, we noticed that the results for strength and those for lifetime scale differently, as can be seen from Tables II to IV. At temperatures $\leqslant 130°$ C the mean strengths of filaments drawn from Spool A are less than or equal to those drawn from Spool B, yet in lifetime, at the same stress ratio, Spool A is superior. To see if this discrepancy was a function of the extreme filament size variability seen in Spool B, we reanalysed the results from Spool B only by dividing the sample groups in half, based upon their measured linear density relative to the median. We observed that for strength, the thick-fibre group slightly exceeded the thin-fibre group; however, the reverse was true for lifetimes, with the thin-fibre group having the somewhat longer lifetime. The magnitude of this shift was roughly equal to $2^{1/s}$, where s is the lifetime shape parameter. As the (mean) volume ratio between filaments in the two groups was approximately 2, it is possible that the lifetime differences are the result of a simple size effect; however, the size effect does not explain the reverse observation for strength.

5. Conclusions

The major conclusions of this study are as follows:

1. Both the strength and creep–rupture lifetime of single Kevlar 49 aramid filaments follow the Weibull distribution. The mean filament strength (and Weibull scale parameter) varies inversely with temperature while the strength variability (and Weibull shape parameter) remains practically constant over the range of temperatures used. Creep–rupture lifetimes show very high variability (small values of the Weibull shape parameter), although at 130° C the variability decreases with decreasing stress level while at 80° C the variability is constant, within experimental error, over the load-range studied.

2. Using the exponential breakdown model with the creep–rupture lifetimes, activation energies in the neighbourhood of 80 kcal mol^{-1} (3.35×10^5 J mol^{-1}) are obtained for the failure process. This activation energy is in line with that required to rupture the C–N bond in the chain backbone, and suggests that chain scission is the dominant mechanism in creep–rupture. However, the time constant obtained using this model

is almost ten orders of magnitude greater than the bond vibrational frequency.

3. For a given yarn spool, filament strength and lifetime seem to be affected slightly differently by increasing temperatures, as illustrated by the relative strengths and lifetimes of filaments drawn from different spools. In lifetime, this difference may be explained by size effects, although for strength there is no obvious explanation.

Acknowledgements

This work was supported in part through funding from the Cornell Materials Science Center, which is funded by the NSF as a DMR-MRL, and in part by a grant from E. I. du Pont de Nemours & Co., Inc. We would like to acknowledge the assistance of Robert Henstenburg, a graduate student in our research group, in the development of the computer programs used with the microprocessor timing circuit, and the MLE analyses.

References

1. S. L. PHOENIX and E. M. WU, Report No. UCRL-53365 (Lawrence Livermore National Laboratory, Livermore, California, 1983).
2. F. P. GERSTLE and S. C. KUNZ, in Proceedings of ASTM Symposium on Long-Term Behaviour of Composites, ASTM STP 813 (American Society for Testing and Materials. Philadelphia, Pennsylvania, 1983) p. 263.
3. H. D. WAGNER, S. L. PHOENIX and P. SCHWARTZ. *J. Comp. Mater.* **18** (1984) 312.
4. H. D. WAGNER, P. SCHWARTZ and S. L. PHOENIX, *J. Mater. Sci.* **21** (1986) 1868.
5. W. I. GRIFFITH, D. H. MORRIS and H. F. BRINSON, in Proceedings of the 3rd International Conference on Composite Materials, Paris, France, August 1980 (Pergamon, Oxford).
6. H. F. BRINSON, D. H. MORRIS and Y. T. YEOW, in Proceedings of the 6th International Conference on Experimental Stress Analysis, Munich, West Germany, 1978, (VDI-Berichte Nr. 3/3, 1978) p. 395.
7. H. F. BRINSON, W. I. GRIFFITH and D. H. MORRIS, in Proceedings of the 4th SESA International Congress on Experimental Mechanics, Boston, USA, 25–30 May 1980 (Society for Experimental Stress Analysis, Brookfield Center, Connecticut, USA) p. 87.
8. E. DEMUTS and P. SHYPRYKEVICH, *Composites* **15** (1984) 25.
9. G. S. SPRINGER, *J. Reinf. Plast. Comp.* **3** (1984) 85.
10. C. C. CHIAO, in Proceedings of 105th AIME Symposium on Failure Modes in Composites (III), Las Vegas, 22–26 February 1976, p. 157.
11. C. C. CHIAO, R. J. SHERRY and N. W. HETHERINGTON, *J. Comp. Mater.* **11** (1977) 79.
12. L. PENN, Report No. UCID-17777 (Lawrence Livermore National Laboratory, Livermore, California, 1978).
13. L. PENN and R. J. SHERRY, Report No. UCRL-79449 (Lawrence Livermore National Laboratory, Livermore, California, 1979).
14. J. COOK, A. HOWARD, N. J. PARRATT and K. D. POTTER, in Proceedings of 3rd Risø International Symposium on Metallurgy and Materials Science: Creep of Composite Materials, Risø, September 1982, p. 193.
15. M. H. LAFITTE and A. R. BUNSELL, *J. Mater. Sci.* **17** (1982) 2391.
16. B. D. COLEMAN, *J. Polym. Sci.* **20** (1956) 447.
17. *Idem, Trans Soc. Rheol.* **1** (1957) 153.
18. B. D. COLEMAN, A. G. KNOX and W. F. McDEVIT, *Text. Res. J.* **28** (1958) 393.
19. R. E. WILFONG and J. ZIMMERMAN, *J. Appl. Polym. Sci., Appl. Polym. Symp.* **31** (1977) 1.
20. H. EYRING, *J. Chem. Phys.* **4** (1936) 283.
21. A. TOBOLSKY and H. EYRING, *ibid.* **11** (1943) 125.
22. B. D. COLEMAN, *J. Appl. Phys.* **27** (1956) 862.
23. S. N. ZHURKOV, *Int. J. Fract. Mech.* **1** (1965) 311.
24. S. N. ZHURKOV and V. E. KORSUKOV, *J. Polym. Sci., Polym. Phys. Edn* **12** (1974) 385.
25. Y. Y. GOTLIB, A. V. DOBRODUMOV, A. M. EL'YASHEVICH and Y. E. SVETLOV, *Sov. Phys. Solid State* **15** (1973) 555.
26. A. V. DOBRODUMOV and A. M. EL'YASHEVICH, *ibid.* **15** (1973) 1259.
27. C. B. HENDERSON, P. H. GRAHAM and C. N. ROBINSON, *Int. J. Fract. Mech.* **6** (1970) 33.
28. R. M. CHRISTENSEN, *Int. J. Fract.* **15** (1979) 3.
29. *Idem, J. Rheol.* **25** (1981) 517.
30. *Idem, Int. J. Solids Struct.* **20** (1984) 791.
31. R. M. CHRISTENSEN and R. E. GLASER, *J. Appl. Mech.* **52** (1985) 1.
32. S. L. PHOENIX, in Proceedings of 9th US National Congress of Applied Mechanics, Book No. H00228, Cornell University, Ithaca, New York, 21–25 June 1982 (American Society of Mechanical Engineers, New York, 1982) p. 219.
33. S. L. PHOENIX and L.-J. TIERNEY, *Eng. Fract. Mech.* **18** (1983) 193.
34. S. L. PHOENIX and C. C. KUO, in "Advances in Aerospace Structures, Materials and Dynamics", edited by U. Yuceoglu, R. L. Sierakowski and D. A. Glasgow, Book No. H00272 (American Society of Mechanical Engineers, New York, 1983) p. 169.
35. S. L. PHOENIX, *Int. J. Fract.* **14** (1978) 327.
36. H. F. WU, PhD thesis, Cornell University (1987).

Received 3 March
and accepted 29 April 1987